Characterization of the Fullerene Derivative [60]PCBM, by High-Field Carbon, and Two-Dimensional NMR Spectroscopy, Coupled with DFT Simulations

Tong Liu,[1] Alston J. Misquitta,[1] and Isaac Abrahams,[2] and T. John S. Dennis[3,4]*

1 School of Physics and Astronomy and Thomas Young Centre for Theory and Simulations of Figure

2 School of Biological and Chemical Sciences and Materials Research Institute, Queen Mary University of London, Mile End Road, London, E1 4NS, UK

3 Department of Polymer Science and Engineering, Zhejiang University, Hangzhou, 310027, China

4 Haina-Carbon Nanostructure Research Center, Yangtze Delta Region Institute of Tsinghua University, Jiaxing, Zhejiang, 314006, China

Abstract: High-resolution (600 MHz) ^{1}H and ^{13}C chemical shift and 2D HETCOR NMR spectra of [60]PCBM were recorded. Resonances from every carbon atom of the ester, phenyl and cyclo-fullerenyl groups, were fully accounted. Assignments of the fullerene cyclopropa-ring, and all phenyl and ester carbons to their respective resonances were based on a HETCOR 2D NMR spectrum. Remaining fullerene assignments were made to a high level of confidence with the aid of an ωB97X hybrid HF/DFT simulation of the ^{13}C NMR spectrum employing a triple zeta Dunning-type basis set. The best result was obtained with the range-separation parameter ω set effectively to zero. This indicates that the fraction of HF in the HF/DFT hybrid at very short range is the dominant factor in achieving good NMR results, that ωB97X with its 15.77% HF fraction at $r_{ij} = 0$ seems very well suited, and that allowing the HF fraction to increase with range is not particularly beneficial. The resulting spectrum had a remarkable qualitative agreement with experiment with a very low mean absolute error for fullerene carbons of 0.09 ppm, which was considerably lower than the 0.28 ppm of the more commonly used B3LYP/6-31G(*d*,*p*) method.

Keywords: Fullerene derivatives, PCBM, NMR, HETCOR, DFT.

1. Introduction

The fullerene derivative methyl 4-[61-phenyl,3'*H*-1,9-cyclo(C_{60}-I_h)[5,6]fullerene-1,9-yl]butanoate is more commonly known as phenyl C_{61} butyric acid methyl ester – or simply by the acronym PCBM. It was first reported by Hummelen, Wudl and co-workers in 1995 as one of six examples of the synthesis of novel homo-bridged and methano-bridged cyclo-additions to the fullerene C_{60}, and identified at the time by the name M1-OMe [1]. Originally intended as a higher-solubility analogue of C_{60}, it is has gone on to be one of the most important n-type molecules in organic electronics; principally as the archetypal electron acceptor in bulk heterojunction photovoltaics [2] and other applications in organic electronics including photodetectors, transistors and light emitting diodes [3-10].

Although ^{13}C line positions of the nuclear magnetic resonance (NMR) spectra of [60]PCBM were reported with the original synthesis [1], the ^{13}C data revealed only 33 resonances from [60]PCBM's 42 chemically inequivalent carbons, with no ^{13}C integration analysis or atom assignments for the fullerene. However, it must be emphasized that the original data were not intended to be a detailed NMR

analysis of what became an important new molecule; but instead, was very successfully provided as reasonable proof-of-synthesis.

In this paper we present high resolution ^{13}C and 2D NMR spectra of the archetypal organic-electronics acceptor material [60]PCBM. Resonances from every carbon atom of the butyric acid methyl ester group, the phenyl group and the fullerene were identified in the ^{13}C spectrum *via* chemical shift and reliable integration analysis. The analysis was informed by a ωB97X DFT simulation of the ^{13}C NMR spectrum employing a triple zeta Dunning basis set. This simulation gave remarkable agreement with experiment, both qualitatively overall and through a very low mean absolute error of 0.09 ppm for the fullerene carbons, which is substantially lower than the 0.28 ppm error obtained for a 'standard' B3LYP/6-31G(*d,p*) simulation. The analysis allowed for the resonances to be assigned to their respective carbon atoms of the fullerene. This was done with full integration analysis allowing for the 4 fullerene atoms on the mirror plane to be identified, such that these may be used as a fingerprint for the benchmarking of other DFT methods. It also unambiguously resolves the atom assignments of all the carbon atoms addend – where there is currently disagreement in the literature with almost no agreement on most assignments.

The chemical shift of each chemically distinguishable carbon nucleus gives a direct indication of the electron density surrounding it. This is because the electron density contributes to the degree of shielding of the otherwise identical nuclei from the static external magnetic field of the NMR spectrometer. Hence, knowing which resonance corresponds to which fullerene carbon atom provides information of the variation of local electron density over the surface of the fullerene. This may provide information on the regio-chemical reactivity of [60]PCBM, which may in turn provide useful information to synthetic organic chemists aiming to functionalise this important molecule – for example, by targeted synthesis of one specific isomer from the 19 possible isomers bis[60]PCBM [11]. It may also contribute to furthering the theory of chemical reactivity in strained organic molecules of which fullerenes are an example.

2. Materials and Methods

[60]PCBM was synthesized *via* an adaption of the original method of Hummelen *et al.* [1] in three steps: (1) esterification of 5-oxo-5-phenylpentanoic acid (methanol reflux); (2) conversion to a tosylhydrazone (reflux with *p*-toluenesulfonyl hydrazine); and (3) anaerobic reaction of the tosylhydrazone with sodium methoxide in pyridine mixed with C_{60} in 1,2-dichlororbenzene under sodium-vapor lamp irradiation at 85°C during 18 h. A two-page step-by-step description of the adaption we used is given open-source in the SI of Liu *et al*. [12]. The as-produced [60]PCBM was purified by preparative high-pressure liquid chromatography (HPLC) in single pass mode (Japan Analytical Industry LC-908 HPLC; Waters Sunfire 19 mm i.d. × 150 mm column; toluene eluent; 18 ml min^{-1} flow rate; UV detection at 312 nm) following the method of Shi *et al*. for bis[60]PCBM isomers [13]. The purification yielded only two products: [60]PCBM and unreacted C_{60}, which were completely separated from one another.[12]

The ^{13}C chemical shift and heteronuclear correlation (HETCOR) 2D NMR spectra were recorded on Bruker AV600 spectrometer in CS_2 solution (5 mm diameter tube) to which a few drops of deuterated benzene signal lock were added. For the ^{13}C NMR measurement, 2048 scans were co-added to yield the final spectra. All ^{13}C peaks were referenced to the d6-benzene lock at 128.06 ppm. Chemical shifts (ppm) are reported to two decimal places (with insignificant errors).

The geometry of [60]PCBM was optimised at the B3LYP/cc-pVTZ level of theory. This was followed by gauge independent atomic orbitals (GIAO) hybrid Hartree-Fock (HF)/Density Functional theory (DFT) method simulations of the ^{13}C NMR spectrum was performed using the Gaussian 16 package [14] (ωB97X [15] range-separated hybrid method coupled with a correlation-consistent polarized valence-only triple zeta (cc-pVTZ) [16] basis set. For this method, the range-separation parameter ω for electron exchange was set to zero $bohr^{-1}$ while the other parameters were kept at their default values. We motivated to vary ω from IP/HOMO matching, which suggested that a much lower value of ω was needed to match the HOMO to the IP of [60]PCBM. However, further investigation suggested best results were obtained by this parameter to zero. For the interested reader, the range separation parameter ω was set to 0.0001 $bohr^{-1}$ (effectively zero) in Gaussian 16 by the following command: "iop(3/74=-57,3/107=0000100000,3/108=0000100000)" – omit the quotation marks. The command "3/74=-57" specifies ωB97X as the hybrid HF/DFT method; "3/107=000010000" sets ω for the long-range DFT exchange to 0.0001 $bohr^{-1}$, and leaves ω for the short-range DFT exchange at its default value (0.3000 $bohr^{-1}$); "3/108=0000100000" plays analogous roles for the long and short range ω for the HF exchange. For comparisons, the ^{13}C NMR spectrum was also simulated with the very commonly used B3LYP/6-31G(*d,p*) [17] method, and by the X3LYP/6-31G [18] method that was recently reported [19] as giving reliable results on similar cyclo-fullerene derivatives, e.g., $C_{61}H_2$ [20]. B3LYP, as the 'standard' DFT technique was used for the geometry optimisation rather than the methods used to simulate the various NMR spectra for reasons of consistency. That is, with a single geometry optimisation for all NMR spectral simulations, the difference in the various ^{13}C NMR simulations is the simulation method (not the geometry or a combination of the two). This may be justified on grounds that a DFT method suitable for the calculation of electron shielding tensors is not necessarily suited for electron energy minimisation *via* iterative structure variation. As such, there is no particular advantage of using the same method but there may be potential disadvantages of doing so.

The atom numbering system used in this paper follows International Union of Pure and Applied Chemistry (IUPAC) recommendations. To aid the interpretation of this papers, a fully numbered diagram of [60]PCBM is given in Figure 1. In this paper, C*x* , C*x*' and C*x*" (where *x* is an integer) is used to refer to the numbering of fullerene, ester and phenyl carbons, respectively; and "C*x*|C*y*" is used to designate symmetrically-equivalent pairs of carbon atoms and "C*x*&C*y*" designates accidental coincidences. The optimized structure of [60]PCBM is given as Supplementary Material (SM.1).

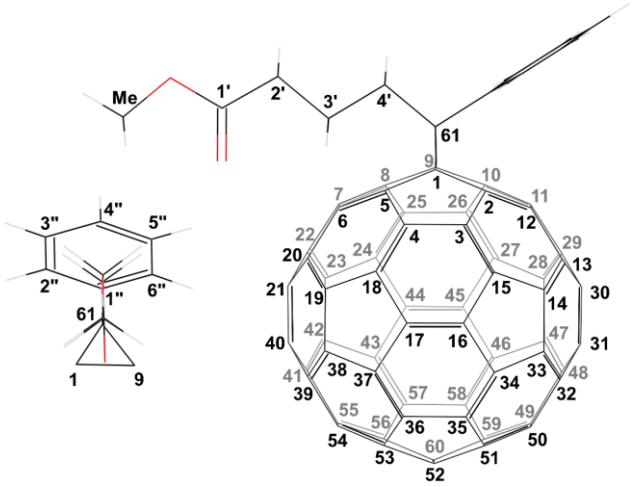

Figure 1: The atom numbering system used in this paper, which follows IUPAC recommendations. The insert on the left shows C1, C9 and C61 that form the cyclopropa ring, together with the carbons of the phenyl ring. For clarity, these are shown rotated 90˚ from the main figure.

3. Experimental Results and Discussion

3.1. HETCOR 2D NMR Spectrum

The 2D, $^{1}H/^{13}C$ NMR, spectrum is given in Figure 2(a) for the aliphatic resonances and 2(b) for the aromatic resonances. The hydrogen resonances from the phenyl group occur at 7.79, 7.41 and 7.33 ppm. The methyl group resonates at 3.50 ppm, and the hydrogens of the C_3H_6 chain occur at 2.8, 2.3 and 2.1 ppm. With this 2D spectrum the hydrogens of phenyl and ester groups may be associated with their respective carbon resonances, as follows: 7.79–132.30 ppm, 7.41–128.79 ppm, 7.34–128.55 ppm, 3.50–51.28 ppm, 2.81–34.05 ppm, 2.34–33.87 ppm and 2.07–22.90 ppm (see Figure 3 and Table 1 below for the ^{13}C resonances).

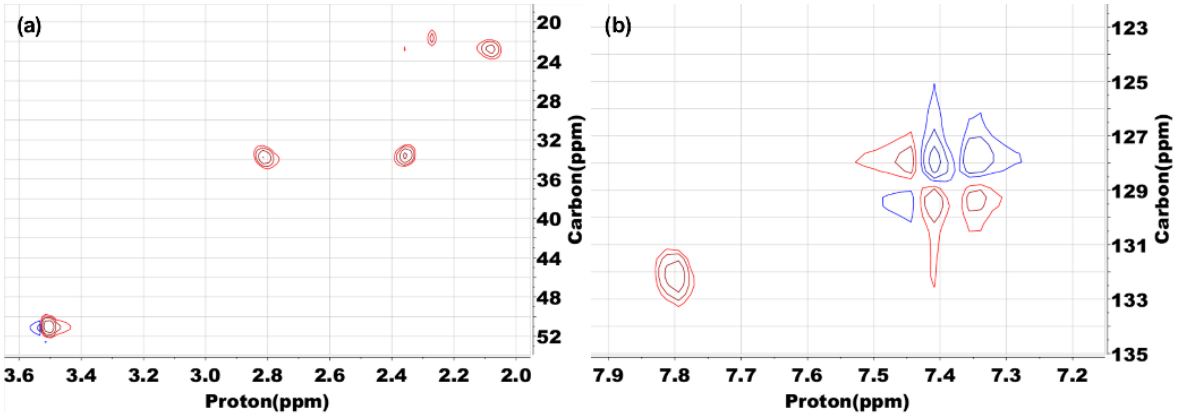

Figure 2. The 2D NMR spectrum of [60]PCBM for (a) the aliphatic and (b) the aromatic resonances. The contours indicate correlations of ^{1}H and ^{13}C resonances.

Based on typical group frequencies, the ^{13}C NMR resonance at 22.90 ppm corresponds to the centre carbon of the C_3H_6 chain. The 2D spectrum indicates resonance corresponds to the ^{1}H NMR resonance at 2.07 ppm. The ^{13}C NMR resonances from the two end-carbons of the C_3H_6 chain, C2' and C4', occur very close together at 33.87 and 34.05 ppm. Indeed, the previous reports by Yang *et al*. [20] and Mens *et al*. [21] did not resolve them and hence, could not determine which is which; and although Hummelen *et al*. [1] did assign them, they were not distinguished. That these are so close in chemical shift is not surprising. This is because they are both bonded to a CH_2 group (ester-C3' in both cases) and a carbon with no attached hydrogens (ester-C4' to fullerene-C61 and ester-C2' to the carbonyl group). Hence, both are in similar chemical environments. However, the difference is enough for them to be distinguished from our 2D spectrum. This spectrum shows that it is the ^{13}C resonance at 34.05 ppm that is associated with the ester-C4', and that resonance at 33.87 pm that is associated with ester-C2'.

The 2D spectrum can also be used to distinguish the cyclo-fullerene bridge carbon (C61) from the methyl carbon (both are predicted to occur near 50 ppm). The 2D spectrum clearly indicates that the resonance at 51.28 ppm is associated with methyl ^{1}H resonance at 3.50 ppm; leaving the 52.19 ppm resonance as being from the bridge carbon (C61). Further evidence in favour of this conclusion comes

from the resonance at 52.19 ppm being of slightly lower intensity than that at 51.28 ppm. A lower intensity is expected from the bridge carbon (C61) by reason of it having no attached hydrogens, which are an additional course of spin-lattice relaxation only available to the methyl carbon. The assignment of the resonance at 51.28 ppm to the methyl group is consistent with the previous report, *via* attached proton test (ATP) NMR spectroscopy, of Mens *et al*. [21] However, Hummelen et al. [1] misassigned the methyl group to the higher of the two resonances near 50 ppm, and Yang et al. [20] assigned the methyl group to a resonance near 62.00 ppm, which is not present in our spectrum.

Turning to the phenyl group, the spectrum shows that the single intensity ^{13}C resonance 128.55 ppm correlates with the ^{1}H resonance at 7.34 ppm, which can only originate from the phenyl-C4" carbon. The two double intensity resonances at 128.79 and 132.30 ppm are respectively associated with the ^{1}H resonances at 7.41 and 7.79 ppm. Hence, it is phenyl carbons C2"|C6" that resonate at 132.30 ppm and C3"|C5" that resonate at 128.79 ppm. This leaves the single intensity ^{13}C resonance at 136.93 ppm as originating from the phenyl carbon with no protons (C1") (which we had already surmised above based on its lower intensity when compared to the other single intensity resonance (128.55 ppm) from phenyl-C4").

3.2. The ^{13}C Spectrum

Figures 3 shows the experimental ^{13}C NMR spectrum of [60]PCBM for (a) the sp^3 hybridized carbons (20 to 83 ppm); (b) the phenyl carbons, which are all sp^2 hybridized (124.5 to 138 ppm); and (c) the fullerene sp^2 carbons (138 to 151 ppm). Also shown as an insert in Figure 3(c) is the resonance from ester carbonyl carbon (near 172 ppm). The full NMR spectrum over the range 0 to 200 ppm is supplied as Supplementary Material (SM.2).

Our ^{13}C NMR data are reasonably consistent with that previously reported [1] with chemical shifts differing by a mean value of +0.64 ppm, with a standard deviation of 0.05 ppm. This discrepancy is mainly due to different reference standards used – C_6D_6 at 128.06 ppm here and CS_2 at 192.5 ppm in Reference [1]. The spectrum presented here allows for resonances for all carbons to be accounted for. This includes reliable integrations which differentiate between singly and doubly degenerate resonances and for accidental coincidences of resonances, which show as integration-3 and integration-4 lines in the experimental spectrum. The previous report [1] did not contain any integration analysis of the fullerene resonances; and there are several resonances, representing 18 carbons, that were not noted. In addition, the C2"|C6" phenyl resonance at 132.30 ppm was misassigned as being from the fullerene.

The ^{13}C NMR spectrum of [60]PCBM indicates 42 chemically distinguishable carbon environments which is only consistent with the molecule having C_S point group symmetry. These resonances include to five resonances from the methyl butanoate group (each of unitary integrated intensity). Of these, four are sp^3 hybridized (C2', C3' and C4') and one is sp^2 hybridized (C1'). There are four resonances from the phenyl group (all sp^2), with phenyl carbons C1" and C4" having single intensity (being on the mirror plane) and the others having double intensity (as C2"|C6" and C3"|C5" are each mirrored pairs).

For the fullerene, there are two possible addition sites that are consistent with C_S symmetry. One of these entails a 1,9,61 cyclopropa-ring and the other a 1,2,61 cyclopropa-ring. However, the 1,2,61 structure can be rejected for several reasons: 1,2 bonding introduces double bonds into pentagons which disrupts the highly-stable single bond – double bond conjugation of the fullerene while simultaneously giving in considerable bonds strain *via* higher bond angle pyramidalization. In addition, the refined crystal structure of [60]PCBM from XRD analysis is 1,9 bonded [21]. In addition, an attempt to optimise the structure of PCBM with a 1,2,61 cyclopropa-ring as the input geometry resulted in an

optimised geometry in which the 1,2 bond was broken with a C1–C2 separation of 2.16 Å – *i.e.*, a homofullerene that was calculated to be 33 kJ mol^{-1} (0.34 eV $molecule^{-1}$) less stable than the 1,9-bonded cyclofullerene structure. Furthermore, the homofullerene would produce a ^{13}C NMR spectrum that is inconsistent with experiment. The input and optimised geometries of this 1,2-bonded isomer are given as Supporting Materials (SM.3). Hence, [60]PCBM is a 1,9,61-cyclofullerene where the four equatorial carbons C21, C30, C31 and C40, the bridge carbon C61, the methyl butanoate group and the phenyl carbons C1" and C4" lie on the mirror plane, and the remainder of the fullerene and phenyl groups are bisected by the plane.

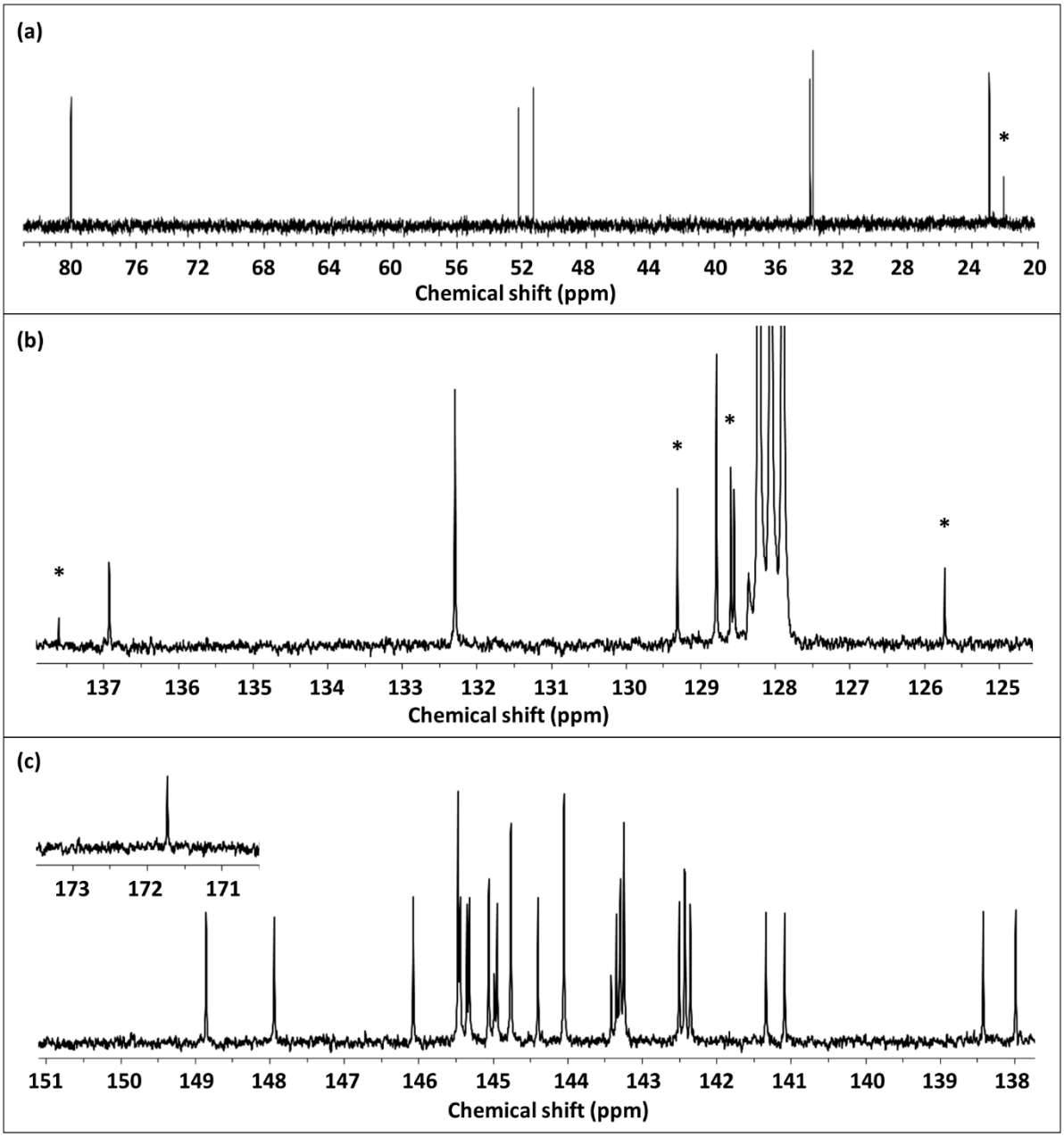

Figure 3. The ^{13}C NMR spectrum of [60]PCBM showing (a) the sp^3, (b) the phenyl, (c) the fullerene resonances (the inset is from the carbonyl). Resonances with an asterisk are from residual toluene tenaciously retained by the sample, and off-scale resonances near 128 ppm in are from the C_6D_6 signal lock**.**

There should be 33 resonances from the cyclo-fullerene. These comprise a single intensity resonance from the bridge (C61), four single intensity resonances, one from each of the four abovementioned equatorial carbons on the mirror plane, and finally, 28 double intensity resonances from those either side of the mirror plane. The cyclo-fullerene resonances result from sp^2 hybridized carbons except for the resonances from (a) the bridge carbon (C61) and the resonance from the two symmetrically equivalent bridgehead carbons (C1 and C9), which are each sp^3 hybridized.

Based on typical group-resonance values, we expect the following qualitative spectrum for [60]PCBM. The sp^2 region (above 120 ppm) should comprise a single intensity line from the carbonyl of the methyl butanoate group near 170 ppm; 31 resonances from the fullerene between 135 and 150 ppm, of which 27 are of double intensity and 4 are of single intensity; and 4 resonances from the phenyl group between 125 and 135 ppm, of which 2 are of single intensity and 2 are of double intensity.

The sp^3 region (below 90 ppm) should comprise a total of 6 resonances. These are, a double intensity resonance from the fullerene bridgehead carbons near 70 ppm, a single resonance from the fullerene bridge carbon near 50 ppm, a single intensity line from the methyl carbon of the methyl butanoate also near 50 ppm, and three single intensity resonances from the C_3H_6 group between 20 and 40 ppm – with the middle carbon having the lowest chemical shift.

In general, the ^{13}C spectrum presented here (Figure 3) is in line with the above prediction. There is a resonance at 171.72 ppm, fullerene lines between 137.95 and 148.83 ppm, 4 phenyl lines between 128.55 and 136.93 ppm, and 6 resonances in the sp^3 region ranging from 80.04 to 22.90 ppm. In the sp^2 region, the resonance at 171.72 ppm is well-separated from the other resonances and is typical of carbonyl carbons. Hence, it is readily assigned to C1' of the methyl butanoate group.

The number of sp^2 fullerene resonances, at 25, is lower than the 31 expected. However, integration analysis indicates that there are several accidental coincidences of lines. The lines at 145.44, 144.72, 144.02 and 143.21 ppm are all of integration 4 – indicating that each is a coincidence of two intrgration-2 lines; and the lines at 145.03 and 143.26 ppm are of integration-3 – both indicating the coincidences of a double and a single integration line. With these analyses, resonances from all 58 sp^2 fullerene carbons are fully accounted for in Figure 4. This includes those of the four single intensity resonances, which originate from the 4 equatorial carbons on the mirror plane (C21, C30, C31 and C40) that occur at 145.03, 144.95, 143.38, and 143.26 ppm.

The 4 resonances from the phenyl carbons are the first four resonances in the sp^2 region, 128.55 (1C), 128.79 (2C), 132.30 (2C), and 136.93 (1C). Three of these resonances ascribed to the phenyl group have intensities greater than expected based on their degeneracy. This behaviour results from faster relaxation of these three ^{13}C nuclei environments (C2"|C6", C3"|C5" and C4") by their attached hydrogens. By this reasoning, the single intensity resonances at 128.55 and 136.93 ppm are respectively assigned to phenyl carbon C4" and C1", on the basis that C4", having an attached hydrogen, has greater intensity. The double degenerate resonances at 128.79 and 132.30 ppm may be respectively assigned to phenyl carbons C3"|C5" and C2"|C6" based on typical group frequencies. In addition, as will be discussed in detail below, the DFT simulations also give this order to the lines and the 2D spectrum confirms these assignments.

In the sp^3 region, the double intensity bridgehead carbons (cyclo-fullerene carbons C1 and C9) appear at 80.04 ppm. The bridge carbon and the methyl carbons appear close together near 52 ppm. Based on the 2D NMR spectrum, it is the resonance at 51.28 ppm that has associated hydrogens (at 3.50 ppm; and hence, this resonance that is assigned to the methyl carbon – leaving the resonance at 52.19 ppm to be assigned to the bridge carbon (C61). The two end carbons (C4 and C2) of the C_3H_6 part of

the methyl butanoate group occur at 34.05 and 33.87 ppm (again, determined *via* the 2D NMR spectrum), and the middle carbon of that chain occurs at 22.90 ppm. The remaining resonances, all from the fullerene, will be analysed in the next section with reference to DFT simulations. A summary of the analysis based on the experimental ^{13}C the 2D spectrum is given in Table 1.

Table 1. The ^{13}C NMR chemical shifts, integrations, and assignment based on the 2D spectrum.

Chemical shift/ppm	Int.	Assignment	Chemical shift/ppm	Int.	Assignment
171.72	1	Ester-C1'	52.19	1	Fullerene-C61
136.93	1	Phenyl-C1"	51.28	1	Methyl
132.30	2	Phenyl-C2"|C6"	34.05	1	Ester-C4'
128.79	2	Phenyl-C3"|C5"	33.87	1	Ester-C2'
128.55	1	Phenyl-C4"	22.90	1	Ester-C3'
80.04	2	Fullerene-C1|C9			

4. DFT Simulation Results and Discussion.

The ^{13}C NMR spectrum of [60]PCBM was simulated by three methods: B3LYP/6-31G(*d*,*p*) as this method is a *de-facto* standard for practically all chemical property calculations, geometry optimisations and spectral simulations; X3LYP/6-31G, which is reported in the literature to gives very low errors for fullerene derivatives [19] and stated to be the best method of simulating the NMR spectra of fullerene-related molecules; and ωB97X/cc-pVTZ, which we found gave exceptionally good results. For the latter method, the range-separation parameter ω was set effectively to zero. We were originally motivated to alter ω based on ionisation potential-tuning which suggested a lower value than the default was required to match the ionisation potential to the highest occupied molecular orbital. However, subsequent systematic testing of simulated ^{13}C NMR spectra led to the effectively-zero value. Figure 4 shows the ^{13}C NMR spectrum of [60]PCBM as simulated by the three methods in comparison to the experimental spectrum. The simulations were all referenced such that their respective first lines (from carbon C3') had the experimental chemical shift (22.90 ppm).

The sp^3 region (Figure 4a) is clearly best represented by ωB97X simulation. This is evident in terms of the overall pattern and chemical shift accuracy. For example, the spacing between the C2' and C4' ester resonances (near 34 ppm) is 0.18 ppm experimentally. The ωB97X simulation quite accurately predicts this gap to be 0.27 ppm. Whereas X3LYP simulates this gap to be far wider at 2.33 ppm, and B3LYP prediction is even wider. Similarly, the spacing between the C61 and methyl carbon (near 52 ppm) is 0.91 ppm experimentally and 0.98 by the ωB97X simulation, 1.54 ppm in the X3LYP simulations and 2.5 ppm in the B3LYP simulations. In addition, the order of the lines agrees with the experimental 2D data, particularly that the methyl carbon has a lower chemical shift than the bridge carbon C61.

In the sp^2 region, Figure 4(b), all three simulation correctly predict that the first four lines should comprise two lines with single degeneracy and two with double degeneracy, and that they correspond to the phenyl carbons. The order of the lines here also agrees with experiment except that the short line from phenyl carbon C4" and the tall line from the mirrored C3"|C5" pair of phenyl carbons are reversed in the ωB97X simulation compare with that of the experiment. However, as the separation of these two resonances is very small, this is not a significant failure. Indeed, the general experimental

features of two very close lines near 128 ppm, a single double intensity lines near 132 ppm and a single intensity line near 137 ppm is, like for the sp^3 region, most accurately predicted in the ωB97X simulated spectrum. Two of these lines, at 132.29 and 136.93 ppm were previously assigned to the fullerene [1]. However, our 2D spectrum shows that these originate from the phenyl. In addition, all three simulations, using three different methods with three different basis sets, agree that these resonances originate from the phenyl group. Before turning to the more complicated fullerene sp^2 resonances it is noted that the three simulations predict that the carbonyl resonance should be near 170 ppm, with again ωB97X being the closest to experiment in Figure 4(d).

One objective measurement that may be used to test the accuracy of simulations is the mean absolute error (MAE). The determination of this for the spectra of the three simulation methods will be discussed in detail later. However, as the results show that ωB97X has the lowest MAE of the three methods by a considerable margin (at 0.09 ppm compared to 0.28 ppm for X3LYP and 0.28 ppm for B3LYP), the remainder of the discussion on the fullerene sp^2 carbons will be based primarily on the ωB97X simulation.

The 58 fullerene sp^2 carbons should give rise to 4 single intensity lines from the 4 carbons on [60]PCBM's mirror plane (C21, C30, C31 and C40) and 27 double intensity lines from the carbons split by the mirror plane. Consulting the experimental spectrum Figure 3(c) reveals that the fullerene resonances occur in separated groups. These groups comprise a pair of lines near 138 ppm representing 4 carbon atoms, a pair of lines representing 4 carbon atoms near 141 ppm, four lines near 142.5 ppm (8 carbons), a group of four lines (10 carbons) near 143 ppm, a wide group of three lines between 144 and 144.8 ppm from 10 carbons, a close group of three lines near 145 ppm from 6 carbons, a cluster of 5 lines from 12 carbons between 145.5 and 146 ppm, and finally a pair of double intensity lines, representing the remaining 4 fullerene sp^2 carbons near 148.5 ppm. Consulting the simulated spectrum reveals the same number of groups of resonances with the same number of carbon atoms in each respective group as that of the experimental spectrum. Furthermore, within each group the distribution of the lines within the group may be matched between the simulated and experimental spectra. With this, we will attempt to assign each line in the experimental spectrum to its corresponding carbon atom(s) *via* comparison of the real and simulated spectra.

The fullerene part of the spectrum begins with two lines, each of integration 2C, that occur at 137.95 and 138.38 ppm. This pair of lines is well separated from the other lines with a spacing of 0.43 ppm. A very similar feature is seen in all three simulated spectra, and all associate them with two mirrored pairs of carbon atoms: C11|C12 and C6|C7. The four members of this pair are all in symmetrically equivalent positions on the C_{61} cyclo-fullerene cage. They are, therefore, split into two lines only through the influence of the asymmetry of the addend. Confidence in this assignment comes from the first fullerene line in the INADEQUATE spectrum of 13% ^{13}C-enriched $C_{61}H_2$ having a very similar chemical shift (136.77 ppm) and originating from these same 4 carbon atoms [20]. The chemical shift order of these two [60]PCBM lines is the same in all three simulations. As will be detailed, discussed and determined later, the mean absolute error (MAE) in the chemical shifts from the ωB97X simulation for the sp^2 fullerene carbons is 0.09 ppm, which is far smaller than the separation of these two lines from each other and from other lines. Hence, as this order is the same on the different DFT methods and different basis sets, and as the spacing between them is more than 4 times the MAE of the qualitatively and quantitatively best simulation, these first two lines are confidently assigned as originating from the two mirrored pairs of carbon atoms C11|C12 and C6|C7 in the order of increasing chemical shift. Additional confidence in this assignment and in the ωB97X simulation comes from the differences between the experimental and simulated spacings between these two lines (at 0.43 ppm and 0.47 ppm, respectively) is only 0.04 ppm.

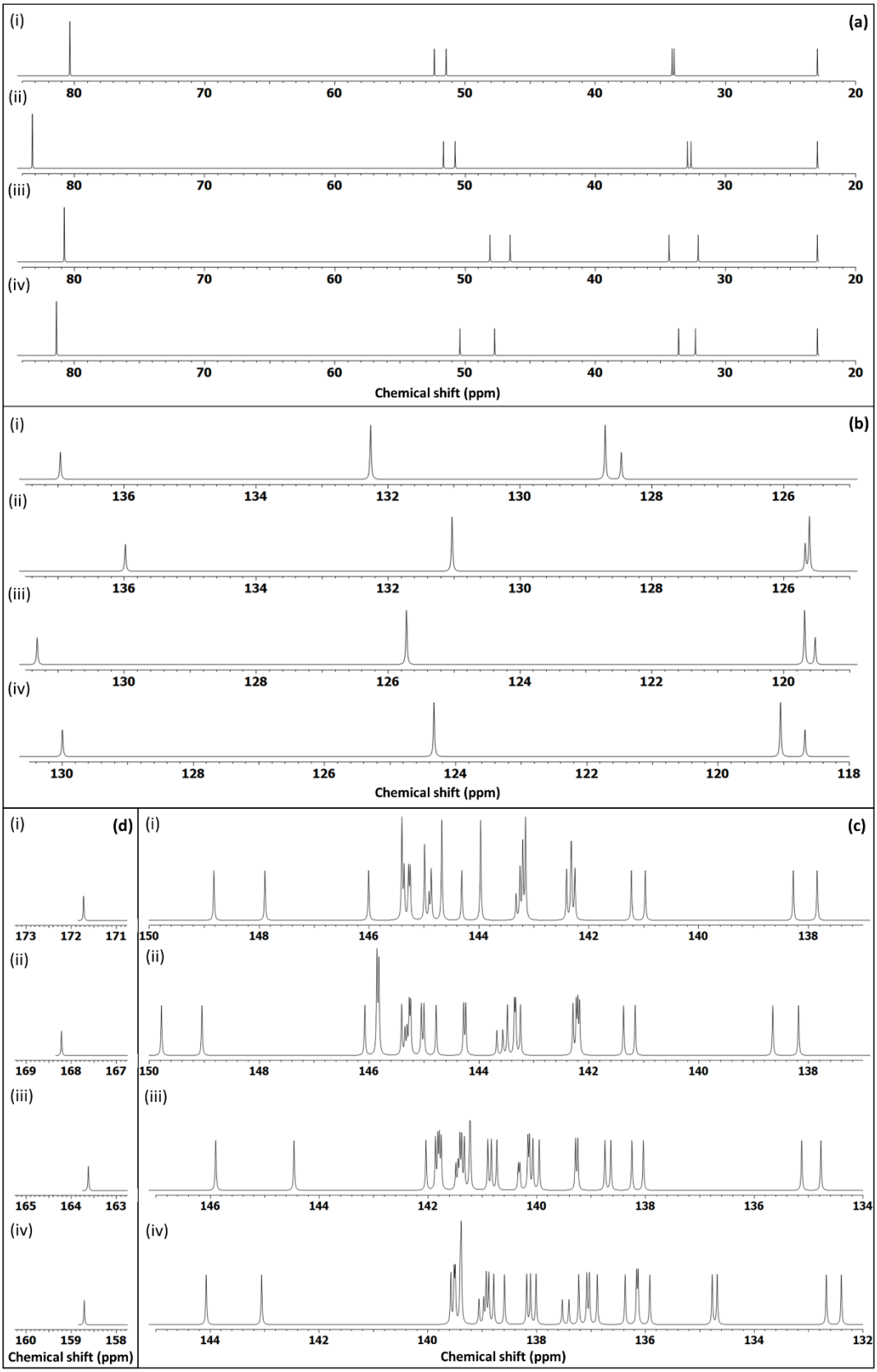

Figure 4. The experimental and simulated ^{13}C NMR spectra for the (a) sp^3 hybridizes carbons, (b) the sp^2 phenyl carbons, (c) the sp^2 fullerene carbons, and (d) the carbonyl carbon. In each case (i) represents the experimental spectrum, and (ii), (iii) and (iv) respectively represent the ωB97X/cc-pVTZ, B3LYP/6-31G(*d,p*) and X3LYP/6-31G simulations.

After a gap of about 2.5 ppm there is another pair of lines with a slightly narrower spacing than the previous pair (141.05 and 141.30 ppm). Again, all three simulated spectra also have this feature and assigns to the carbons C15|C27 and C18/C24, respectively. As with the previous pair, these 4 carbons are in symmetrically equivalent positions on the fullerene and split into two mirrored pairs through the addend's asymmetry. The closer spacing of this 2nd pair of lines is likely to result from C15|C18|C24|C27 being further from the bridge carbon (C61) than C6|C7|C11|C12. There may also be an effect from C6|C12 and C7|C11 being only about 0.7 Å from the mirror plane of [60]PCBM (being bonded together across it, and hence, being almost directly beneath the addend); whereas, C15|C18 and C27|C24 are about 3.0 Å from that plane. We are confident in these assignments for the same reason given for the first two lines (same order across all DFT/basis set combinations, the spacing is greater than the MAE and that the 2nd line in the ^{13}C-enriched spectrum of $C_{61}H_2$ at 140.98 ppm is assigned to these 4 carbons [20]). As with the previous pair of lines, the ωB97X simulation has very accurately predicted the spacing (0.04 ppm difference).

After a gap of 1.02 ppm there is then a cluster of 4 lines spread over 0.14 ppm. These all have integration 2C. However, the two central lines are separated by only 0.01 ppm and give the appearance of a single line of enhanced intensity. This feature as very accurately reproduced in the ωB97X simulated spectrum, which assigns them in the order C20|C22 (142.32 ppm), C13|C29 (142.38 ppm), C34|C46 (142.39 ppm) and C37|C43 (142.47 ppm). The next 2 resonances in the spectrum of $C_{61}H_2$ [20] correspond to these same 8 carbons and appear in the same order as that of the ωB97X simulation (as C34|C46|C37|C43 at 142.24 ppm and C13|C29|C20|C22 at 142.78 ppm). Hence, we are very confident that the 8 carbons in this cluster are indeed fullerene carbons C13, C20, C22, C29, C34, C37, C43 and C46. However, as the chemical shift range of this cluster (0.15 ppm) is commensurate the MAE of the ωB97X simulation (0.09 ppm), it appears that the line order cannot be assigned with high confidence. As such, although we are confident of the membership of this cluster of resonance from 8 carbons, based on the small chemical shift range of this cluster in both the experimental and ωB97X simulated spectra, the resonances are only tentatively assigned to their corresponding carbon atoms.

Following a gap of 0.74 ppm there is a close cluster of 4 lines, between 143.21 and 143.48 ppm, from 10 carbon atoms (with integrations of 4C, 3C, 2C and 1C). The first of these lines (143.21 ppm) results from an accidental coincidence of two mirrored pairs of carbon atoms. The next line (143.26 ppm) results from the coincidence of a mirrored pair of carbon atoms and one of the 4 equatorial carbons that lie on [60]PCBM's mirror plane. There then follows a single mirrored pair of carbons (143.31 ppm), and the final line (143.38 ppm) results from another one of the equatorial carbons on the mirror plane. The two equatorial carbons C31 and C40 are spaced by 0.12 ppm, which is wider than the MAE = 0.09 of the ωB97X spectrum which placed them in the order of C40 followed by C31. In addition, that spacing is quite accurately reproduced in the ωB97X simulation (at 0.10 ppm). Hence, we are confident that one of the two resonance at 143.26 ppm and the resonance at 143.38 ppm respectively correspond to C40 and C31. The bonds between the equatorial carbons on the mirror plane of [60]PCBM are both vertical, and it is interesting to note that the carbons that are furtherer from the addend (i.e., C31 and C40) have the greater amount of shielding from the applied magnetic field of the instrument.

The remaining double-intensity lines of this cluster are the off-mirror equatorial carbons (C16|C45 and C17|C44) and (C35|C58 and C36|C57) from all simulations. This cluster of 10 atoms in the spectrum of $C_{61}H_2$ [20] shows as two lines: one at 143.02 ppm from carbons C35|C58|C36|C57 (which is coincident with the resonances from C31 and C40 already discussed), and a line at 143.15 ppm from the 4 horizontal equatorial carbons C16|C45|C17|C44. These pairs are opposite each other on the

same hexagonal ring (the ring C17, C16, C34, C35, C36 and C37), and the C16 and C35 are both bonded to the other member of their pair (C17 and C36, respectively). The simulated spectra suggest that the components of the two pairs have separated chemical shifts. Hence, the accidental coincidence of quadruple intensity is more likely to come from a coincidence of the first member of each pair rather than two members of the same pair. Furthermore, the gap differences of these four resonances are narrower than MAE of ωB97X. Hence, it tentatively assigns the line at 143.21 ppm to C17|C44 and C36|C57. It follows from this discussion that the double intensity component of the triple intensity line at 143.26 ppm may be tentatively assigned to carbons C35|C58. This leaves the double intensity line at 143.31 ppm as tentatively assigned to the equatorial carbons C16|C45.

The next three lines in the spectrum occur at 144.02, 144.36 and 144.72 ppm and have integrations of 4C, 2C and 4C. These lines have considerably greater spacing than the MAE in the ωB97X simulation, and hence, may be assigned with some confidence. This is particularly true as this series of lines is well represented in the ωB97X simulated spectrum. The main difference is that the 1st and 3rd lines appear as pairs of lines with a very small splitting in the simulation, whereas the experimental spectrum shows these two lines as coincidence. They are assigned in the simulated spectrum to carbons (C33|C47&C38|C42), (C14|C28), and (C49|C50&C54|C55), respectively in order of increasing chemical shift. Further confidence in these assignments comes from the experimental spectrum of $C_{61}H_2$, which has resonances from these same carbons in the same order as the next three lines in its spectrum.[9] It is interesting to note that the first 4C-integration line corresponds to carbons that would be in symmetrically equivalent positions on the fullerene, C33, C38, C42 and C47, but for the asymmetry of the addend. The same can be said of the 2nd 4C-integration line (from C49|C50|C54|C55). However, the equivalent pair for C14|C28 is widely split from its equivalent (C19|C23). It was suggested earlier that the very wide splitting of C6|C7 from C11|C12 and the slightly narrower spacing of C18|C24 from C15|C27 was related to the distance from the addend. The present three resonances agree with this suggestion. The widely spaced C14|C28 and C19|C23 resonances result from carbon pairs on the same hemisphere as the addend, whereas the other two 4C-integration lines with zero splitting are on the opposite hemisphere.

The next feature in the experimental spectrum is a cluster of three lines between 144.91 and 145.03 ppm from 6 carbons, with integrations of 2C, 1C and 3C in order of increasing chemical shift. The last line represents a coincidence of an integration 1 and an integration 2 resonance Amongst these must be the resonances from the two remaining equatorial carbons on the molecule's mirror plane (C21 and C30). Comparison with the experimental spectrum of $C_{61}H_2$ [20], suggests that the remaining two resonances originate from the polar C52|C60 mirrored pair; as these correspond to the next two non-equatorial resonances so far unaccounted for in that spectrum. Confidence in that conclusion comes from the ωB97X simulation which indicates this cluster comprises C52|C60, C19|C23, C30 and C21 in order of increasing chemical shift. The calculated gaps between the two ingegration-2 carbons are less than the MAE of the simulation, as are those between the two integration-1 carbons. Hence, although we are confident in the carbon atom membership of this cluster of lines, we cannot decide from the calculation on the C52|C60 and C19|C23 line order, or on the C21 and C30 line order. However, it is noted that C52|C60 comes after C19|C23 in the experimental spectrum of $C_{61}H_2$ [20] and in the B3LYP and X3LYP simulated spectra of [60]PCBM; and that the ωB97X simulation has these two resonances as almost coincident (0.02 ppm separation), and hence, as mentioned above ambiguous on line order. However, if we consider the ωB97X simulation in relation to the splitting caused by the asymmetry of the addend; it quite accurately predicts all the other confidently assignable splittings. For example, the splitting of C6|C7|C11|C12 into C6|C7 and 11|C12 is calculated to be 0.47 ppm, which compares well to the experimental splitting of 0.43 ppm; and the experimental splitting of C15|C27|C18|C24 is

0.25 ppm, which again compares well with the simulated splitting of 0.21 ppm. With the line at 144.36 ppm confidently assigned to C14|C28, if we add the 0.48 ppm simulated splitting by the asymmetry from C19|C23 we get 144.84 ppm. The only integration-2 line close to this is at 144.91 ppm (0.07 ppm away). The only reasonable alternative is the integration-3 line at 145.03 ppm, which gives an atypically large splitting by the asymmetry of 0.19 ppm away from experiment (where 0.04 ppm is typical). In addition, a simulated splitting difference from experiment of 0.07 ppm is within the MAE of the simulation, whereas, 0.19 ppm is a considerably larger splitting than the simulation error would suggest. Hence, the integration-2 resonance at 144.91 much more likely corresponds to C19|C23, leaving the integration-2 component of the line at 145.03 to come from C52|C60. With none of the three simulation being inconsistent with this conclusion, these assignments are confidently made. The remaining two unassigned carbons in this cluster are the equatorial carbons C21 and C30, which must originate from the resonances at 144.95 and 145.03 ppm. These resonances are tentatively assigned to C30 and C21, respectively, based on the ωB97X simulation order.

There then follows a cluster of 5 lines of integrations 2C except for the 4th line which is of integration 4C. Comparison with the experimental spectrum of $C_{61}H_2$ [20] suggest that these originate from: (a) C32|C39|C41|C48, which being just below the equator of C_{60} are expected to split narrowly into C32|C48 and C39|C41; (b) C51|C53|C56|C59, which are the 2nd-most distant set of atoms from the addend (being bonded to the polar carbon are expected to show very little, if any, splitting into C51|C59 and C53|C56 mirrored pairs; and (c) C3|C4|C25|C26, which are on the same pentagon as the addend, and hence, expected to be widely split on [60]PCBM into C3|C26 and C4|C25 mirrored pairs. Based on this, it is likely that the 4C integration line at 145.44 ppm results from a coincidence of C51|C59 and C53|C56 virtually unsplit mirrored pairs; the resonances at 145.32 and 145.40 ppm result from C32|C48 and C39|C41 narrowly split mirrored pairs; and the resonances at 145.29 and 146.04 ppm result from C3|C26 and C4|C25 widely split mirrored pairs. Some confirmation of this from the ωB97X simulation which shows that the last line originates from C4|C25 and the first from C3|C26 – a widely split pair as predicted. Not only is in line with the above discussion, the separation of these resonances from the others in this cluster is significantly greater than the MAE of the simulation. Hence, these 4 carbons may be confidently assigned to their corresponding resonances in the experimental ^{13}C NMR spectrum. However, the ωB97X simulation does not quite correspond to the above analysis for the remaining lines. The simulation shows these as a set of two accidental coincidences, with C32|C48 being coincident with C53|C56 and C39|C41 coincident with C51|C59. However, the double accidental coincidence makes such pairings highly unlikely. That is, (1) it suggests that C51|C59 and C53|C56 (which are closest to the pole) have the same splitting by the asymmetry of the other addend as do C32|C48 and C39|C41(which are closest to the equator) when there appears to be a trend of the splitting increasing as the distance between the two addends decreases; and (2) C51|C59 (near the pole) has the same chemical shift as C32|C48 (near the equator). Based on this analysis, the resonances at 145.29 and 146.04 ppm are confidently assigned to C3|C26 and C4|C25, respectively. The resonances at 145.32 and 145.40 ppm are tentatively assigned to C32|C48 and C39|C41, in simulation order, and the integration 4C resonance at 145.44 ppm is equally tentatively assigned to C51|C59 and C53|C56.

The final feature in the spectrum for the fullerene sp^2 carbons is a pair of well separated lines at 147.91 and 148.83 ppm. The spectrum of $C_{61}H_2$ [20] suggests that these originate from the splitting of one resonance (from C2, C5, C8 and C10) into two mirrored pairs through the asymmetry of the addend. The simulation suggests that they correspond to C5|C8 and C2|C10 in order of increasing chemical shift. The wide splitting and high chemical shifts are expected. The wide splitting comes from these being the 4 closest sp^2 fullerene carbons to the addend (as discussed above), and the high chemical shift comes from them being the 4 carbons bonded to the only two sp^3 hybridized on the fullerene

(the two bridgehead carbons – C1 and C9). With this, the resonances at 147.91 and 148.83 ppm are assigned with a high degree of confidence to C5|C8 and C2|C10, respectively. A full list of all fullerene sp^2 resonances together with their integrations and assignments based on the above discussion are presented in Table 2. This table also lists the corresponding ωB97X calculated chemical shifts and their difference from experiment.

Table 2. The experimental ^{13}C NMR chemical shifts, integrations and atom assignments for the fullerene sp^2 carbons of [60]PCBM based on the conclusion of ^{13}C NMR spectroscopy and ωB97X/cc-pVTZ DFT simulation. Assignments in bold are confidently made owing to close resemblances to the experimental spectrum, while the others are only tentatively assigned based on the ωB97X simulated spectrum.

Expt. (ppm)	Int	Calc. (ppm)	Expt – Calc.	Assignment	Expt. (ppm)	Int	Calc. (ppm)	Expt. – Calc.	Assignment
137.95	2	138.00	-0.05	**C11/C12**	144.36	2	144.53	-0.17	**C14/C28**
138.38	2	138.46	-0.08	**C6/C7**	144.72	2	144.75	-0.03	**C54/C55**
141.05	2	140.94	0.11	**C15/C27**	144.72	2	144.80	-0.08	**C49/C50**
141.30	2	141.15	0.15	**C18/C24**	144.91	2	145.02	-0.11	**C19/C23**
142.32	2	141.95	0.37	C20/C22	144.95	1	145.06	-0.11	**C30**
142.38	2	141.98	0.40	C13/C29	145.03	2	145.09	-0.06	**C52/C60**
142.39	2	142.01	0.38	C34/C46	145.03	1	144.99	0.04	**C21**
142.47	2	142.06	0.41	C37/C43	145.29	2	145.15	0.14	C3/C26
143.21	2	143.01	0.20	C36/C57	145.32	2	145.56	-0.24	C32/C48
143.21	2	143.10	0.11	C17/C44	145.40	2	145.57	-0.17	C39/C41
143.26	2	143.33	-0.07	C35/C58	145.44	2	145.60	-0.16	C53/C56
143.26	1	143.12	0.14	**C40**	145.44	2	145.60	-0.16	C51/C59
143.31	2	143.25	0.06	C16/C45	146.04	2	145.82	0.22	**C4/C25**
143.38	1	143.44	-0.06	**C31**	147.91	2	148.76	-0.85	**C5/C8**
144.02	2	144.00	0.02	**C38/C42**	148.83	2	149.49	-0.66	**C2/C10**
144.02	2	144.04	-0.02	**C33/C47**					

5. Accuracy of the Simulations

In the above discussion the 58 sp^2 hybridized fullerene carbons were assigned based on the DFT simulations of the spectrum. One objective measurement that may be used to test the accuracy of simulations is the MAE. This parameter measures the mean of the absolute difference between each of the observes and calculated chemical shifts of the molecule. This method requires the knowledge of the assignments in the experimental spectrum. But in the case of [60]PCBM, these are technically do not know. However, as mentioned above, the areas of qualitative subjective agreement between experiment and simulation, coupled with some chemical knowledge, may lead to reasonably confident assignments.

To test the objective accuracy of the DFT simulations a table was drawn up of the above-made confident qualitative assignment together with their corresponding simulated values. In order to draw the meaningful conclusions, the simulated spectra were each re-referenced with the aim of minimizing the MAE for each method. This was done in order to minimize the effect of the arbitrariness of referencing. Re-referencing does not in any way alter the form of the spectrum; as the number of lines, their relative intensities and there spacings all remain identical. It merely shifts the entire spectrum up or down by a constant.

Re-referencing was done as follows. First, another table was drawn up of the chemical shifts of the confidently assigned fullerene carbons from each of the three simulations. Second, a value of $\delta_{exp}–\delta_{calc}$ was then obtained for each carbon from each method. Third, these values were averaged for each

simulation methods. Finally, each of the three simulated spectra were then re-referenced by shifting them by their corresponding average difference. In this way the new re-referenced δ_{exp}–δ_{calc} values will be the result of inconsistencies between experiment among each of the simulations. The corresponding values are presented in Table 3 from which the following MAEs were obtained: sp^2-$MAE_{\omega B97X}$ = 0.09 ppm, sp^2-MAE_{X3LYP} = 0.28 ppm and sp^2-MAE_{B3LYP} = 0.28 ppm based on the confident fullerene sp^2 atoms assignments.

The subjective assessment that the ωB97X simulation bore a remarkable resemblance to the experimental spectrum for the complex fullerene sp^2 carbons part of the spectrum reflected in it having by far the lowest MAE of the three methods. Taking the value for the MAE of the ωB97X simulation, the tentative assignments were re-examined. However, none of these assignments became any less tentative. This is because all previous 'confident assignments' had spacing considerably greater than the MAE, where all 'tentative assignments' had spacings commensurate with of lower than the MAE.

Table 3. Table of experimental and simulated chemical shifts and their absolute differences and mean absolute error (MAE) for each simulation method against initial confident fullerene carbon atom assignments.

Expt (ppm)	Atom Assignment	ωB97X	Exp-Cal	X3LYP	Exp-Cal	B3LYP	Exp-Cal
137.95	C11/C12	138.01	0.06	138.14	0.19	138.50	0.55
138.38	C6/C7	138.47	0.09	138.49	0.11	138.77	0.39
141.05	C15/C27	140.95	0.10	141.38	0.33	140.76	0.29
141.3	C18/C24	141.16	0.14	141.59	0.29	140.85	0.45
143.31	C40	143.34	0.03	143.65	0.34	143.58	0.27
143.38	C31	143.45	0.07	143.63	0.25	143.46	0.08
144.02	C38/C42	144.01	0.01	144.15	0.13	144.16	0.14
144.02	C33/C47	144.05	0.03	144.21	0.19	144.06	0.04
144.36	C14/C28	144.54	0.18	144.05	0.31	144.23	0.13
144.72	C54/C55	144.76	0.04	144.64	0.08	144.83	0.11
144.72	C49/C50	144.81	0.09	144.72	0.00	144.97	0.25
145.29	C3/C26	145.16	0.13	144.54	0.75	144.92	0.37
146.04	C4/C25	145.83	0.21	145.34	0.70	145.43	0.61
MAE			**0.09**		**0.28**		**0.28**

The reason for why ωB97X performed particularly well when compared to the other methods cannot be attributed to the range separation aspects of this method. This is because the agreement between calculation and experiment increased for this method as the range separation parameter ω decreased, with the best agreement occurring when ω was set effectively to zero. Setting ω to zero turns off range separation meaning that the ratio of HF and DFT contributions to the electron exchange energy is effectively constant with electron pair separation over the whole of size of the molecule. As such ωB97X exchange behaves in the same manner as B3LYP and X3LYP with electron pair separation. This leaves the X in ωB97X as the major factor in the accuracy of the calculation – which is the full-range HF coefficient. This coefficient, c_X, is 0.1577 in ωB97X and higher at 0.2000 in B3LYP [17] and 0.2180 in X3LYP [18] and 0.2100 in B97-1 [22]. It is also higher in the closely related ωB97XD at 0.2220 [15]. With this, ^{13}C NMR spectra were also simulated by the ωB97XD and B97-1 methods. A figure with the experimental fullerene sp^2 resonances together with those calculated by ωB97X, ωB97XD, B97-1 is supplied in the Supplementary Material (SM.4). From this it may be concluded that lowering the HF contribution to the hybrid from the typical default values of 0.2 to about 0.15 results in increases accuracy. However, a further reduction to the zero of a pure DFT method decreases accuracy. As such,

it may be concluded that the selection of a hybrid HF/DFT method with a suitable ratio of HF and DFT may increase the accuracy of ^{13}C NMR spectral simulations.

5. Conclusions

In conclusion, high resolution ^{13}C and 2D NMR spectra of the archetypal organic-electronics acceptor material [60]PCBM were recorded. Resonances from every carbon atom of the butyric acid methyl ester group, the phenyl group and the fullerene were identified in the ^{13}C spectrum *via* chemical shift and reliable integration analysis.

A 2D-dimensional NMR spectrum allowed for assignments of all carbons with attached hydrogens to their respective resonances. By a process of elimination, the fullerene sp^3 carbons, bridgehead carbons (C1 and C9) and the bridge carbon (C61), were also unambiguously assigned. This spectrum resolves the substantial conflict in the literature on these line assignments.

The chemical shifts of [60]PCBM and the simulation thereof to assign resonances to their respective carbon atoms yields experimental information on local electron densities over the surface of the fullerene, and thereby provides novel information on the electronic structure of this highly important molecule to the field of organic electronics.

An ωB97X DFT simulation (with ω set to zero) of the ^{13}C NMR spectrum employing a triple zeta Dunning basis set gave remarkable agreement with experiment, both qualitatively overall and through a very low mean absolute error of 0.09 ppm for the fullerene carbons. This was substantially lower than the 0.28 ppm error obtained for a standard B3LYP/6-31G(*d,p*). As such, the remaining fullerene resonances, and the ester carbonyl resonance were assigned to their respective resonances to a reasonable level of confidence. The ability to confidently make these assignments suggests that this computational combination is highly suited for the simulation of the ^{13}C NMR spectra of fullerene derivatives.

The simulation indicated that the 'standard' B3LYP method is not necessarily an appropriate method for ^{13}C NMR calculations. Our investigation suggests that ωB97X, with ω set to zero gives excellent results. In addition, as setting ω to zero turns off range separation, this indicates that it is the full-range HF coefficient is crucial to obtaining good results. These findings are not confined to fullerene derivatives; they are of general applicability in organic chemistry. As such, the judicial selection of an appropriate hybrid calculation method followed by tuning its HF/DFT ratio may lead to greatly improved ^{13}C NMR spectrum simulations of all organic molecules.

Author contributions: The manuscript was written through contributions of all authors. TL synthesized and purified the [60]PCBM. IA facilitated access to the NMR spectrometer and aided TL and TJSD in the data analysis. AJM aided TL and TJSD with the performance and analysis of the DFT simulations. TJSD, AJM and IA co-supervised TL; and TL and TJSD wrote the paper. All authors have given approval to the final version of the manuscript.

Funding: This research required no external funding.

Acknowledgements: This research utilised Queen Mary's Apocrita HPC facility, supported by QMUL Research-IT (http://doi.org/10.5281/zenodo.438045). We also thank the China Scholarship Council and QMUL for a joint PhD studentship to Tong Liu; Dr Harold Toms of the School of Biological and Chemical Sciences at QMUL for assistance with recording the NMR spectra.

Conflict of interest: The authors declare no conflict of interest.

References

[1] J.C. Hummelen, B.W. Knight, F. LePeq, F. Wudl, J. Yao, C.L. Wilkins, Preparation and Characterization of Fulleroid and Methanofullerene Derivatives, Journal of Organic Chemistry 60 (1995) 532-538.

[2] P.R. Berger, M. Kim, Polymer solar cells: P3HT: PCBM and beyond, Journal of Renewable and Sustainable Energy 10(1) (2018).

[3] T. Ameri, P. Khoram, J. Min, C.J. Brabec, Organic Ternary Solar Cells: A Review, Advanced Materials 25(31) (2013) 4245-4266.

[4] C.L. Chochos, N. Tagmatarchis, V.G. Gregoriou, Rational design on n-type organic materials for high performance organic photovoltaics, Rsc Advances 3(20) (2013) 7160-7181.

[5] B.C. Thompson, Y.G. Kim, T.D. McCarley, J.R. Reynolds, Soluble narrow band gap and blue propylenedioxythiophene-cyanovinylene polymers as multifunctional materials for photovoltaic and electrochromic applications, Journal of the American Chemical Society 128(39) (2006) 12714-12725.

[6] C. Xie, F. Yan, Enhanced performance of perovskite/organic-semiconductor hybrid heterojunction photodetectors with the electron trapping effects, Journal of Materials Chemistry C 6(6) (2018) 1338-1342.

[7] Z. Tang, Z.F. Ma, A. Sanchez-Diaz, S. Ullbrich, Y. Liu, B. Siegmund, A. Mischok, K. Leo, M. Campoy-Quiles, W.W. Li, K. Vandewal, Polymer: Fullerene Bimolecular Crystals for Near-Infrared Spectroscopic Photodetectors, Advanced Materials 29(33) (2017).

[8] X. Zhao, T. Liu, X. Hou, Z. Liu, W. Shi, T.J.S. Dennis, 60 PCBM single crystals: remarkably enhanced band-like charge transport, broadband UV-visible-NIR photo-responsivity and improved long-term air-stability, Journal of Materials Chemistry C 6(20) (2018) 5489-5496.

[9] D. Jarzab, K. Szendrei, M. Yarema, S. Pichler, W. Heiss, M.A. Loi, Charge-Separation Dynamics in Inorganic-Organic Ternary Blends for Efficient Infrared Photodiodes, Adv. Funct. Mater. 21(11) (2011) 1988-1992.

[10] G.J. Zhao, Y.J. He, Z. Xu, J.H. Hou, M.J. Zhang, J. Min, H.Y. Chen, M.F. Ye, Z.R. Hong, Y. Yang, Y.F. Li, Effect of Carbon Chain Length in the Substituent of PCBM-like Molecules on Their Photovoltaic Properties, Advanced Functional Materials 20(9) (2010) 1480-1487.

[11] T. Liu, I. Abrahams, T.J.S. Dennis, Structural Identification of 19 Purified Isomers of the OPV Acceptor Material bisPCBM by C-13 NMR and UV-Vis Absorption Spectroscopy and High-Performance Liquid Chromatography, Journal of Physical Chemistry A 122(16) (2018) 4138-4152.

[12] T. Liu, I. Abrahams, T.J.S. Dennis, Conformational Analysis of [60]PCBM via Second-Order Proton NMR Spin−Spin Coupling Effects, Journal of Physical Chemistry Letters 11 (2020) 5397-5401.

[13] W. Shi, X. Hou, T. Liu, X. Zhao, A.B. Sieval, J.C. Hummelen, T.J.S. Dennis, Purification and electronic characterisation of 18 isomers of the OPV acceptor material bis- 60 PCBM, Chemical Communications 53(5) (2017) 975-978.

[14] M.J. Frisch, G.W. Trucks, H.B. Schlegel, G.E. Scuseria, M.A. Robb, J.R. Cheeseman, G. Scalmani, V. Barone, G.A. Petersson, H. Nakatsuji, X. Li, M. Caricato, A.V. Marenich, J. Bloino, B.G. Janes-ko, R. Gomperts, B. Mennucci, H.P. Hratchian, J.V. Ortiz, A.F. Izmaylov, J.L. Sonnenberg, D. Williams-Young, F. Ding, F. Lipparini, F. Egidi, J. Goings, B. Peng, A. Petrone, T. Henderson, D. Ranasinghe, V.G. Zakrzewski, J. Gao, N. Rega, G. Zheng, W. Liang, M. Hada, M. Ehara, K. Toyota, R. Fukuda, J. Hasegawa, M. Ishida, T. Nakajima, Y. Honda, O. Kitao, H. Nakai, T. Vreven, K. Throssell, J.A. Montgomery, Jr., J.E. Peralta, F. Ogliaro, M.J. Bearpark, J.J. Heyd, E.N. Brothers, K.N. Kudin, V.N. Staroverov, T.A. Keith, R. Kobayashi, J. Normand, K. Raghavachari, A.P. Rendell, J.C. Burant, S.S. Iyengar, J. To-masi, M. Cossi, J.M. Millam, M. Klene, C. Adamo, R. Cammi, J.W. Ochterski, R.L. Martin, K. Morokuma, O. Farkas, J.B. For-esman, D.J. Fox, Gaussian 16, Revision C.01, Gaussian Inc., Wallingford CT, 2016.

[15] J.D. Chai, M. Head-Gordon, Optimal operators for Hartree-Fock exchange from long-range corrected hybrid density functionals, Chemical Physics Letters 467(1-3) (2008) 176-178.

[16] T.H. Dunning, Gaussian-Basis Sets for use in Correlated Molecular Calculations .1. The Atoms Boron Through Neon and Hydrogen, Journal of Chemical Physics 90(2) (1989) 1007-1023.

[17] A.D. Becke, Density-functional exchange-energy approximation with correct asymptotic behavior, Physical Review A 38 (1988) 3098.
[18] X. Xu, Q.S. Zhang, R.P. Muller, W.A. Goddard, An extended hybrid density functional (X3LYP) with improved descriptions of nonbond interactions and thermodynamic properties of molecular systems, J. Chem. Phys. 122(1) (2005) 014105.
[19] A.R. Tulyabaev, I.I. Kiryanov, I.S. Samigullin, L.M. Khalilov, Are there reliable DFT approaches for C-13 NMR chemical shift predictions of fullerene C-60 derivatives?, International Journal of Quantum Chemistry 117(1) (2017) 7-14.
[20] M.S. Meier, H.P. Spielmann, R.G. Bergosh, M.C. Tetreau, Trends in chemical shift dispersion in fullerene derivatives. Local strain affects the magnetic environment of distant fullerene carbons, Journal of Organic Chemistry 68(20) (2003) 7867-7870.
[21] M.T. Rispens, A. Meetsma, R. Rittberger, C.J. Brabec, N.S. Sariciftci, J.C. Hummelen, Influence of the solvent on the crystal structure of PCBM and the efficiency of MDMO-PPV:PCBM 'plastic' solar cells, Chemical Communications (17) (2003) 2116-2118.
[22] F.A. Hamprecht, A.J. Cohen, D.J. Tozer, N.C. Handy, Development and assessment of new exchange-correlation functionals, The Journal of Chemical Physics 109(15) (1998) 6264-6271.

Characterization of the Fullerene Derivative [60]PCBM, by High-Field Carbon, and Two-Dimensional NMR Spectroscopy, Coupled with DFT Simulations

Tong Liu,[1] Alston J. Misquitta,[1] and Isaac Abrahams,[2] and T. John S. Dennis[3,4]*

1 School of Physics and Astronomy and Thomas Young Centre for Theory and Simulations of Materials, Queen Mary University of London, Mile End Road, London, E1 4NS, UK

2 School of Biological and Chemical Sciences and Materials Research Institute, Queen Mary University of London, Mile End Road, London, E1 4NS, UK

3 Department of Polymer Science and Engineering, Zhejiang University, Hangzhou, 310027, China

4 Haina-Carbon Nanostructure Research Center, Yangtze Delta Region Institute of Tsinghua University, Jiaxing, Zhejiang, 314006, China

SUPPLEMENTARY MATERIAL

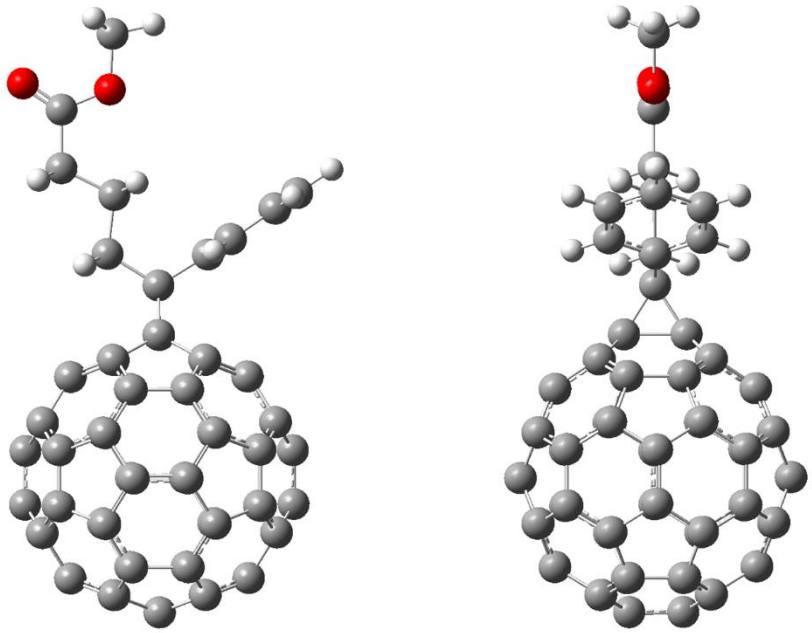

SM.1 The B3LYP/cc-pVTZ optimized structure of [60]PCBM shown in two orientations.

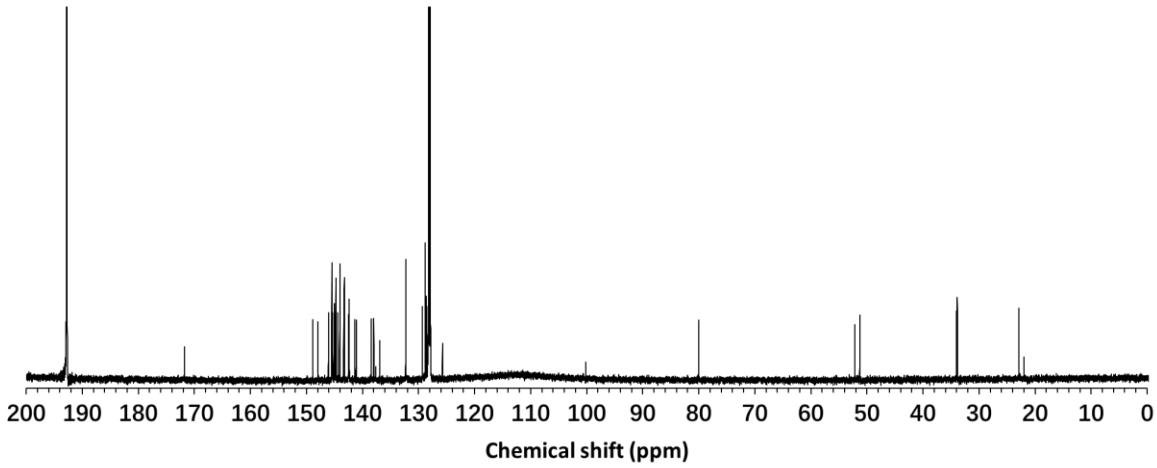

SM.2. The full experimental ^{13}C NMR spectrum of [60]PCBM from which Figure 3 in the paper is constructed. The two off-scale peaks at 128 and 192 ppm respectively correspond to the signal lock (d6-benzene) and the solvent (CS_2).

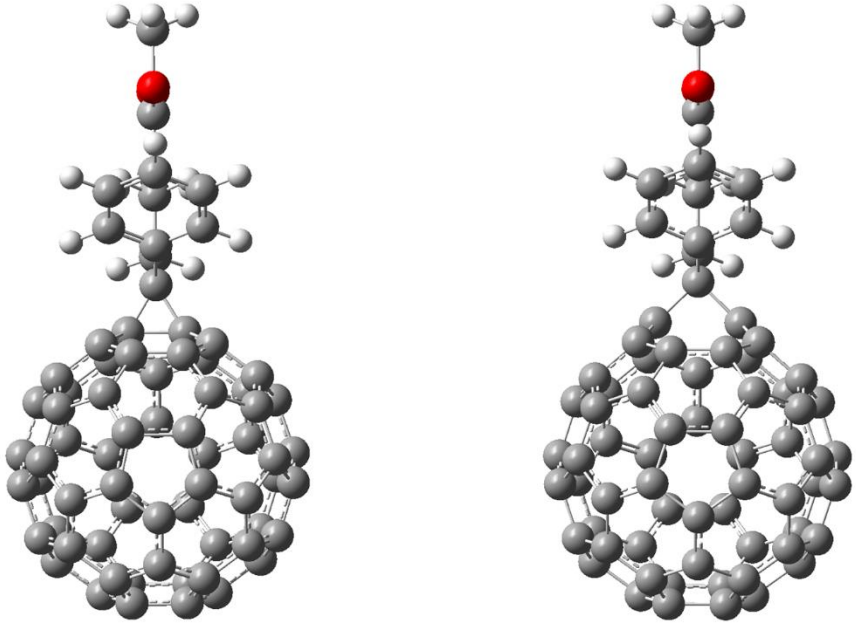

SM.3. The 1,2-bonded cyclofullerene input geometry (left) which optimised to the 1,2-bonded homofullerene (right). The C1-C2 separation is 2.16 Å clearly indicating that the 1,2 bond is broken upon optimisation. As the cyclofullerene optimised to a homofullerene, and as a homofullerene would produce an ^{13}C NMR spectrum that is inconsistent with the experiment, a 1,2-bonded cyclofullerene may be rejected as a possible structure for [60]PCBM. This leaves the 1,9-bonded cyclofullerene as the only possible structure.

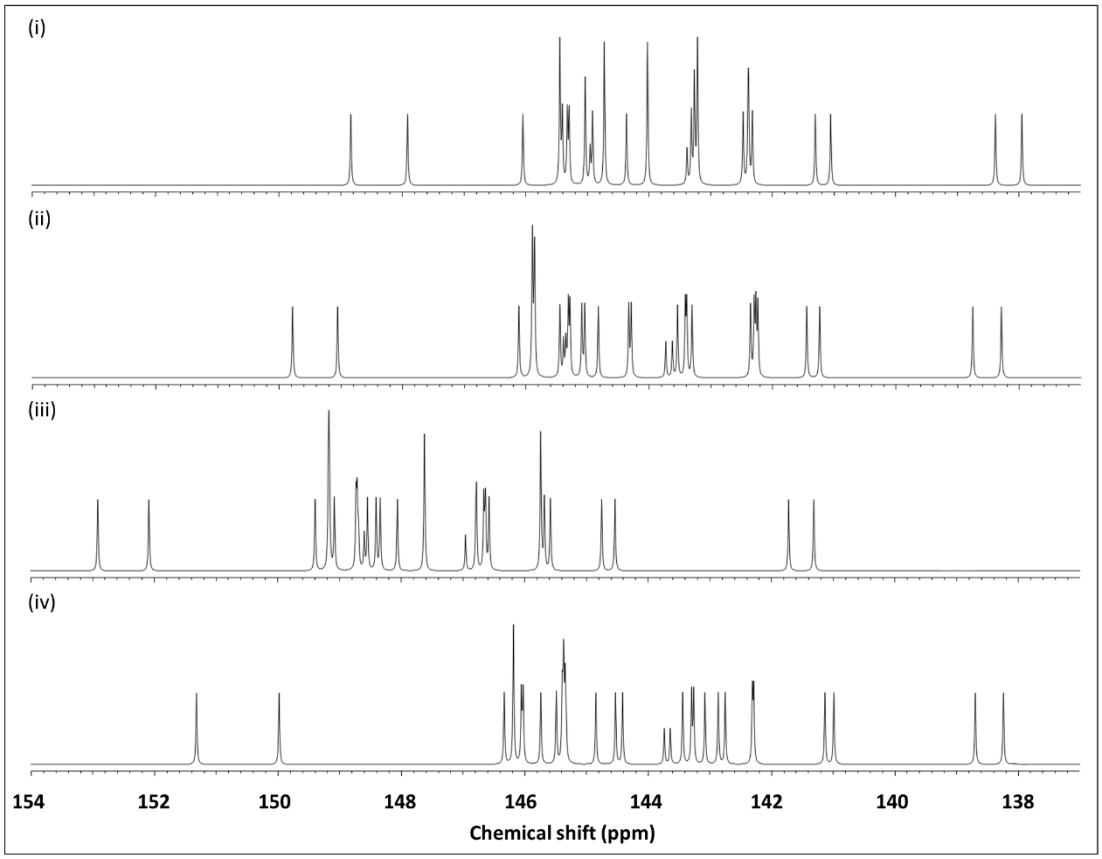

SM.4 The (i) experimental spectrum, (ii) ωB97X simulation with ω = 0.0001 bohr^{-1}, (iii) ωB97XD simulation with ω = 0.0001 bohr^{-1}, and (iv) B97-1 simulation of the sp^2 fullerene carbons of [60]PCBM. In all cases there is no range separation. ωB97X with its relatively low HF contribution to exchange of 15.77% performs best, ωB97XD with its 22.20% contribution fares less well – being similar to B3LYP, 20.00%, X3LYP, 21.80%, and B97-1, 21.00% contribution.